Int. J. Heat Mass Transfer. Vol. 17, pp. 681–691. Pergamon Press 1974. Printed in Great Britain

COMBINED FORCED AND FREE CONVECTION MHD CHANNEL FLOW IN ENTRANCE REGION

H. K. YANG* and C. P. YU
Faculty of Engineering and Applied Sciences, State University of New York at Buffalo, Buffalo, New York 14214, U.S.A.

(*Received* 17 *July* 1973 *and in revised form* 24 *October* 1973)

Abstract—The entrance problem of convective magnetohydrodynamic channel flow between two parallel plates subjected simultaneously to an axial temperature gradient and a pressure gradient is investigated numerically. Both constant heat flux and constant wall temperature cases are considered. The solutions match to the fully developed solutions after a certain entrance length. It is found that an applied transverse magnetic field may reduce the entrance length of the velocity considerably, but has little effect on the temperature development. At high Hartmann number, the velocity entrance length is inversely proportion to M^2 as it was predicted by Shercliff in the absence of free convection. However, a sufficient large free convection may prolong the developing process considerably.

NOMENCLATURE

B, magnetic field;
b, nondimensional induced magnetic field;
B_0, applied magnetic field;
C, constant defined by equation (29);
c, specific heat;
E, electric field;
e, electric field parameter, E_0/V_mB_0;
E_0, constant electric field;
Ec, Eckert number, KV_m^2/cLq or $V_m^2/c(T_w-T_0)$;
g, gravitational acceleration;
Gr, Grashof number, $\beta gL^4q/Kv$ or $\beta gL^3(T_w-T_0)/v^2$;
K, thermal conductivity;
k_1, k_2, constants defined by equation (30);
L, half-width of the channel;
M, Hartmann number, $B_0L(\sigma/\mu)^{1/2}$;
N, Number of divisions in the x direction;
Nu, Nusselt number, $\left(\frac{\partial\theta}{\partial x}\right)_{x=1}\Big/(\theta_w-\theta_m)$;
P, pressure;
p, nondimensional pressure;
Pr, Prandtl number, v/α;
q, heat flux per unit area;
Re, Reynolds number, V_mL/v;
T, temperature;
U, velocity, X-direction;
u, nondimensional form of U;
V, velocity, Y-direction;
v, nondimensional form of V;
V_m, average velocity, $\frac{1}{L}\int_0^L V\,dx$;
X, coordinate, perpendicular to the channel;
Y, coordinate, axial direction;
x, y, nondimensional forms of X, Y;
y_e, entrance length.

Greek letters

α, thermal diffusivity;
β, thermal expansion coefficient;
θ, nondimensional temperature defined in the text;
θ_m, mean nondimensional temperature, $\int_0^1 \theta v\,dx$;
μ, absolute viscosity;
μ_e, magnetic permeability;
ν, kinematic viscosity;
ρ, mass density;
σ, electrical conductivity.

Subscripts

i, at ith position along x-direction;
j, at jth position along y direction;
0, entrance condition, reference condition;
w, wall condition;
x, y, z, scalar components in x, y, z direction.

*Presently at Combustion Engineering, Inc., Chattanooga, Tenn.

INTRODUCTION

THE PROBLEM of combined forced and free convection MHD flow in a vertical channel has been extensively investigated in the fully developed flow region [1–8]. In this paper, we study the development of such flow in the entrance region between two parallel plates. The objective of this study is to examine the effects of the applied magnetic field, free convection and dissipations on the velocity and temperature development, and determine the entrance lengths at various situations.

For the case of a purely forced convection, the entrance problem has been investigated by several authors. Due to the nonlinear inertia terms in the momentum equation, all solutions obtained to date have been approximate solutions. Five different approaches have been used.

The first effort to estimate the MHD entrance length was made by Shercliff [9, 10]. He considered a linear transient problem, in which the velocity varies with time instead of with axial distance. The calculated setting time in the linear problem is then converted to entrance length by multiplying with the mean velocity of flow. He found that for large M where boundary layer approximation applies, the entrance lengths are proportional to ReL/M^2 for parallel plates and to ReL/M for rectangular channel and circular pipe where Re and M denote the Reynolds number and Hartmann number respectively and L is the characteristic length. This method is not precise. The details of the flow for the transient problem would not be expected to agree with the flow in the actual steady-state entrance problem.

In the second approach, the entrance region is divided into an upstream and downstream zone. The upstream zone is assumed of boundary layer formulation. The downstream is described as a perturbation of the fully developed solution. The solution of the entrance region is then obtained by matching the two solutions. This technique was first developed by Schlichting [11] and was applied to the magnetic case by Roidt and Cess [12]. Saric and Touryan [13] also used this method in their work.

The third approach is the momentum integral boundary-layer analysis previously developed by Karman-Pohlhausen. Dhanak [14], Maciulaitis and Loeffler [15], Moffat [16], Hsia [17] and also reference [13] used this approach to MHD problems.

The fourth method involves a linearization of the inertia terms by introducing a stretched coordinate in the direction of flow. It was introduced in the non-magnetic case by Sparrow, Lin and Lundgren [18] and applied to the MHD flow by Snyder [19], Chen and Chen [20] and Hwang [21].

The fifth approach is the numerical technique. The governing equations are written in finite difference form and then solved them on computer. Shohet [22], Shohet, Osterle and Young [23], Hwang and Fan *et al.* [24–27], Flores and Recuers [28] all used this method to solve the entrance problem under different conditions.

In this work, the problem of combined forced and free convection magnetohydrodynamic channel flow in the entrance region will be studied numerically. Using the boundary layer approximation, the parabolic equations are solved as an initial value problem. Both the constant heat flux and constant wall temperature boundary conditions are studied. At the entrance section, however, only the parabolic velocity profile is considered, although the method can handle any other form of entrance velocity profiles.

PROBLEM FORMULATION

Consider an incompressible, viscous and electrically conducting fluid flowing between two parallel vertical plates due to an axial temperature gradient and a pressure gradient. A uniform magnetic field B_0 is applied transversely to the channel. We employ a cartesian coordinate system with Y along the vertical direction, X along the direction of the applied magnetic field. For a steady state, laminar flow under the standard Boussinesq approximation, the equations of continuity, X- and Y- momentum, energy, magnetic induction and state are, respectively,

$$\frac{\partial U}{\partial X}+\frac{\partial V}{\partial Y}=0 \tag{1}$$

$$\rho\left(U\frac{\partial U}{\partial X}+V\frac{\partial U}{\partial Y}\right)=-\frac{\partial P}{\partial X}+\mu\left(\frac{\partial^2 U}{\partial X^2}+\frac{\partial^2 U}{\partial Y^2}\right)+\left[\frac{1}{\mu_e}(\nabla\times\bar{B})\times\bar{B}\right]_x \tag{2}$$

$$\rho\left(U\frac{\partial V}{\partial X}+V\frac{\partial V}{\partial Y}\right)=-\left(\frac{\partial P}{\partial Y}+\rho g\right)+\mu\left(\frac{\partial^2 V}{\partial X^2}+\frac{\partial^2 V}{\partial Y^2}\right)+\left[\frac{1}{\mu_e}(\nabla\times\bar{B})\times\bar{B}\right]_y \tag{3}$$

$$\rho c\left(U\frac{\partial T}{\partial X}+V\frac{\partial T}{\partial Y}\right)=K\left(\frac{\partial^2 T}{\partial X^2}+\frac{\partial^2 T}{\partial Y^2}\right)+\frac{1}{\sigma\mu_e^2}(\nabla\times\bar{B})^2+\mu\left[2\left(\frac{\partial U}{\partial X}\right)^2+2\left(\frac{\partial V}{\partial Y}\right)^2+\left(\frac{\partial V}{\partial X}+\frac{\partial U}{\partial Y}\right)^2\right] \tag{4}$$

$$\nabla^2\bar{B}+\sigma\mu_e\nabla\times(\bar{V}\times\bar{B})=0 \tag{5}$$

$$\rho=\rho_0[1-\beta(T-T_0)] \tag{6}$$

where the last two terms in equation (4) are the Joulean and viscous dissipation.

In order to simplify the problem, we make the following assumptions: (1) the walls are electrically insulating and thermally conducting; (2) small magnetic Reynolds

number, i.e. the induced magnetic field is negligible in comparison with the applied field; (3) the Prandtl boundary-layer approximation applies.

For a two-dimensional flow under assumption (1), we can easily show from Maxwell's equations and Ohm's law that $B_z = 0$ and $E_z = \text{const.} = E_0$. Furthermore, assumption (2) implies that the variation of the transverse magnetic field B_r is small. Thus B_x can be replaced by the constant applied magnetic field B_0. With this in mind, equations (1)–(4) under the boundary layer approximation are reduced to

$$\frac{\partial U}{\partial X}+\frac{\partial V}{\partial Y}=0 \tag{7}$$

$$U\frac{\partial V}{\partial X}+V\frac{\partial V}{\partial Y}=-\frac{1}{\rho_0}\left(\frac{\mathrm{d}P}{\mathrm{d}Y}+\rho_0 g\right)+\beta g(T-T_0)+\nu\frac{\partial^2 V}{\partial X^2}+\frac{\sigma B_0}{\rho_0}(E_0-B_0V) \tag{8}$$

$$U\frac{\partial T}{\partial X}+V\frac{\partial T}{\partial Y}=\alpha\frac{\partial^2 T}{\partial X^2}+\frac{\nu}{c}\left(\frac{\partial V}{\partial X}\right)^2+\frac{\sigma}{\rho_0 c}(E_0-B_0V)^2 \tag{9}$$

where equation (6) has been used.

Equations (7)–(9) are supplemented by the condition

$$\int_{-L}^{L} V\,\mathrm{d}x = 2LV_m = \text{constant} \tag{10}$$

to determine U, V, T and P uniquely, where V_m is the average axial velocity of the flow.

We introduce the following dimensionless parameters:

$$x=\frac{X}{L},\qquad y=\frac{\frac{Y}{L}}{Re}=\frac{\nu Y}{L^2V_m},\qquad v=\frac{V}{V_m}$$

$$u=\frac{URe}{V_m}=\frac{UL}{\nu},\qquad p=\frac{(P-P_0)+\rho_0 gY}{\rho_0 V_m^2},\qquad Re=\frac{V_mL}{\nu}$$

$$M=B_0L\left(\frac{\sigma}{\mu}\right)^{1/2},\qquad Pr=\frac{\nu}{\alpha},\qquad e=\frac{E_0}{V_mB_0}$$

and

$$\theta=\begin{cases}\dfrac{K(T-T_0)}{Lq} & \text{(for constant heat flux)}\\[2ex] \dfrac{T-T_0}{T_w-T_0} & \text{(for constant wall temperature)}\end{cases}$$

$$Gr=\begin{cases}\dfrac{\beta gL^4q}{K\nu^2} & \text{(for constant heat flux)}\\[2ex] \dfrac{\beta gL^3(T_w-T_0)}{\nu^2} & \text{(for constant wall temperature)}\end{cases}$$

$$E_c=\begin{cases}\dfrac{KV_m^2}{CLq} & \text{(for constant heat flux)}\\[2ex] \dfrac{V_m^2}{C(T_w-T_0)} & \text{(for constant wall temperature).}\end{cases}$$

Equations (7)–(10) take form

$$\frac{\partial u}{\partial x}+\frac{\partial v}{\partial y}=0 \tag{11}$$

$$u\frac{\partial v}{\partial x}+v\frac{\partial v}{\partial y}=-\frac{\mathrm{d}p}{\mathrm{d}y}+\frac{Gr}{Re}\theta+\frac{\partial^2 v}{\partial x^2}+M^2(e-v) \tag{12}$$

$$u\frac{\partial\theta}{\partial x}+v\frac{\partial\theta}{\partial y}=\frac{1}{Pr}\frac{\partial^2\theta}{\partial x^2}+E_c\left(\frac{\partial v}{\partial x}\right)^2+M^2E_c(e-v)^2 \tag{13}$$

$$\int_0^1 v\,\mathrm{d}x = 1. \tag{14}$$

The boundary conditions for this problem are

$$\begin{cases}u=0,\ v=0\\ \dfrac{\partial\theta}{\partial x}=1 \quad\text{or}\quad \theta=1\end{cases}\qquad \text{at}\quad x=1,\ y\geqslant 0 \tag{15}$$

$$u=0,\ \frac{\partial v}{\partial x}=0,\ \frac{\partial\theta}{\partial x}=0\qquad \text{at}\quad x=0,\ y\geqslant 0 \tag{16}$$

where equation (16) is obtained by the symmetry conditions about the center line. The condition for θ in equation (15) may be either constant heat flux or constant wall temperature. In addition, we need to prescribe initial conditions for the flow. These are:

$$\begin{cases}v=\frac{3}{2}(1-x^2),\ u=0\\ p=0,\qquad\quad \theta=0\end{cases}\qquad \text{at}\quad 0\leqslant x\leqslant 1,\ y=0. \tag{17}$$

Here the entrance velocity is assumed to have a parabolic profile.

NUMERICAL ANALYSIS

Equations (11)–(14) with conditions (15)–(17) are solved numerically by a finite difference method.

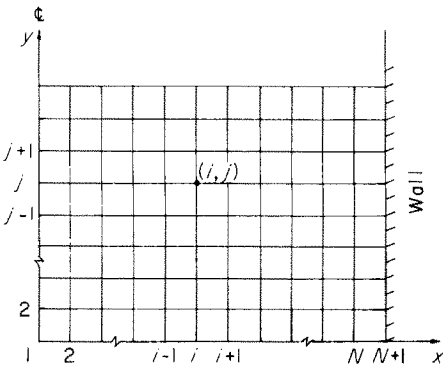

FIG. 1. Mesh network for difference equations.

Considering the mesh net work of Fig. 1, the transverse coordinate can be expressed by

$$x = \frac{i-1}{N} \qquad i = 1, 2, \ldots, N+1$$

$$\Delta x = \frac{1}{N}$$

and all the variables and their derivatives at point (i, j) can be written in the standard finite difference form. Upon substitution, equations (11)–(17) become, respectively,

$$u_{i+1,j} - u_{i,j} = \left[\frac{1}{2\Delta y N}(v_{i+1,j-1} + v_{i,j-1} - v_{i+1,j} - v_{i,j})\right] \quad (18)$$

$$\left[\frac{N}{2}u_{i,j-1} - N^2\right]v_{i+1,j} + \left[2N^2 + \frac{v_{i,j-1}}{\Delta y} + M^2\right]v_{i,j} - \left[\frac{N}{2}u_{i,j-1} + N^2\right]v_{i-1,j} + \left[\frac{1}{\Delta y}\right]p_j = \left[\frac{(v_{i,j-1})^2}{\Delta y} + \frac{p_{j-1}}{\Delta y} + \frac{Gr}{Re}\theta_{i,j} + M^2 e\right] \quad (19)$$

$$\left[\frac{N}{2}u_{i,j-1} - \frac{N^2}{Pr}\right]\theta_{i+1,j} + \left[\frac{v_{i,j-1}}{\Delta y} + \frac{2N^2}{Pr}\right]\theta_{i,j} - \left[\frac{N}{2}u_{i,j-1} + \frac{N^2}{Pr}\right]\theta_{i-1,j} = \left[\frac{1}{\Delta y}v_{i,j}\theta_{i,j-1} + M^2 E_c(e - v_{i,j-1})^2 + \frac{E_c N^2}{4}(v_{i+1,j-1} - v_{i-1,j-1})^2\right] \quad (20)$$

$$v_{1,j} + 4\sum_{k=1}^{\frac{N}{2}} v_{2k,j} + 2\sum_{k=1}^{\frac{N}{2}-1} v_{2k+1,j} = 3N \quad (21)$$

$$\begin{cases} u_{N+1,j} = 0, & v_{N+1,j} = 0 \\ \theta_{N+1,j} = \theta_{N,j+\frac{1}{N}} & \text{or} \quad \theta_{N+1,j} = 1 \end{cases} \quad (22)$$

$$\begin{cases} u_{1,j} = 0, \quad v_{2,j} = v_{0,j}, \quad \theta_{2,j} = \theta_{0,j}, \\ v_{i,1} = \frac{3}{2}\left[1 - \left(\frac{i-1}{N}\right)^2\right] \end{cases} \quad (23)$$

$$u_{i,1} = \frac{M^2}{2}\left[1 - \left(\frac{i-1}{N}\right)^2\right]\ln\left(\frac{1 + \frac{i-1}{N}}{1 - \frac{i-1}{N}}\right),$$

$$\theta_{i,1} = 0, \quad p_1 = 0 \quad (24)$$

where Simpson's formula has been used in writing equation (21).

The sequence of the computation is as follows: starting from the entrance, the energy equation (20) is solved first. Momentum equation (19) and the integral form of continuity equation (21) are then solved simultaneously. Finally, the value of u is obtained from equation (18). These procedures are iterated, until a required accuracy is achieved. Then we proceed to the next step. The equations are linearized in such a manner that whenever the product of two unknowns occurs, one of them is given approximately by its previous known value.

The numerical calculations were performed on a CDC 6400 digital computer. The mesh size for different Hartmann numbers are listed in Table 1.

Table 1. Mesh size for computer computation

Step No.	Step size y	No. of mesh point in x, N	x
		$M < 10$	
1–4	0·0001	80	$1{\cdot}25 \times 10^{-2}$
5–20	0·0002	40	$2{\cdot}5 \times 10^{-2}$
21–40	0·0004	40	$2{\cdot}5 \times 10^{-2}$
41–80	0·0008	20	$5{\cdot}0 \times 10^{-2}$
81 up	0·0016	20	$5{\cdot}0 \times 10^{-2}$
		$10 \leqslant M \leqslant 50$	
1–4	0·00005	80	$1{\cdot}25 \times 10^{-2}$
5–10	0·0001	80	$1{\cdot}25 \times 10^{-2}$
11–20	0·0002	40	$2{\cdot}5 \times 10^{-2}$
21 up	0·0004	40	$2{\cdot}5 \times 10^{-2}$
		$M = 100$	
1–4	0·00001	80	$1{\cdot}25 \times 10^{-2}$
5–10	0·00002	80	$1{\cdot}25 \times 10^{-2}$
11–20	0·00004	40	$2{\cdot}5 \times 10^{-2}$
21–40	0·00008	40	$2{\cdot}5 \times 10^{-2}$
41 up	0·00016	40	$2{\cdot}5 \times 10^{-2}$

The computation is stopped when both the velocity and temperature at the center line reach 1 per cent of their respective fully developed values. The solutions of the fully developed flow for $Ec = 0$ are given by the following expressions. For constant heat flux case

$$v = C(\cosh k_2 \cosh k_1 x - \cosh k_1 \cosh k_2 x) \quad (25)$$

$$\theta - \theta_w = C\left[\frac{\cosh k_2}{k_1^2}(\cosh k_1 x - \cosh k_1) - \frac{\cosh k_1}{k_2^2}(\cosh k_2 x - \cosh k_2)\right]. \quad (26)$$

For constant wall temperature case

$$v = \frac{M}{\cosh M(\tanh M - M)}(\cosh Mx - \cosh M) \quad (27)$$

$$\theta = 1 \quad (28)$$

where

$$C = \left(\frac{\cosh k_2 \sinh k_1}{k_1} - \frac{\cosh k_1 \sinh k_2}{k_2}\right)^{-1} \quad (29)$$

$$k_{1,2}^2 = \frac{M^2}{2} \pm \left(\frac{M^4}{4} - \frac{Gr}{Re}\right)^{1/2}. \quad (30)$$

Having determined the velocity and temperature profiles at each step, the mean temperature, defined by

$$\theta_m = \int_0^1 v\theta \, dx \tag{31}$$

can be calculated by the use of Simpson's rule as follows

$$\theta_m = \frac{1}{3N}\left(\theta_{1,j}v_{1,j} + 4\sum_{k=1}^{\frac{N}{2}} \theta_{2k,j}v_{2k,j} + 2\sum_{k=1}^{\frac{N}{2}-1} \theta_{2k+1,j}v_{2k+1,j}\right). \tag{32}$$

The skin friction and Nusselt's number and the wall temperature are approximated by

$$\left.\frac{\partial v}{\partial x}\right|_{x=1} = \frac{N}{2}(v_{N-1,j} - 4v_{N,j}) \tag{33}$$

$$Nu = \frac{1}{\theta_w - \theta_m}\left.\frac{\partial \theta}{\partial x}\right|_{x=1} = \frac{1}{\theta_w - \theta_m}\frac{N}{2}(\theta_{N-1,j} - 4\theta_{N,j} + 3),$$

$$\theta_w = 1 \quad \text{(for constant wall temperature)} \tag{34}$$

$$\theta_w = \theta_{N+1,j} = \tfrac{1}{3}\left(4\theta_{N,j} - \theta_{N-1,j} + \frac{2}{N}\right), \quad Nu = \frac{1}{\theta_w - \theta_m}$$

(for constant heat flux). (35)

RESULTS AND DISCUSSION

The numerical calculations were performed on a CDC 6400 digital computer. The results for both constant heat flux and constant wall temperature cases are obtained.

(A) *Developing velocity and temperature profiles of the constant heat flux case*

The developing velocity and temperature profiles for different parameters are illustrated in Figs. 2–5. In Fig. 2, the developing velocity and temperature profiles are plotted for $M = 4$, $Gr/Re = 10$ and $Pr = e = 1$, $Ec = 0$. In this case, the velocity profiles have the form not too differently from the non-magnetic isothermal velocity profile. When Gr/Re becomes large and free convection is important a central core is developed in which the velocity is smaller than that of the surrounding as shown in Fig. 3 where $Gr/Re = 100$.

Figure 4 shows the developing velocity and temperature profiles for $M = 100$. The Hartmann effect on the velocity is readily seen and the distance needed to develop the flow is much shorter than the nonmagnetic case. However, the magnetic field has only a minor effect on the development of temperature profiles. The entrance length for the temperature field is little affected by the magnetic field.

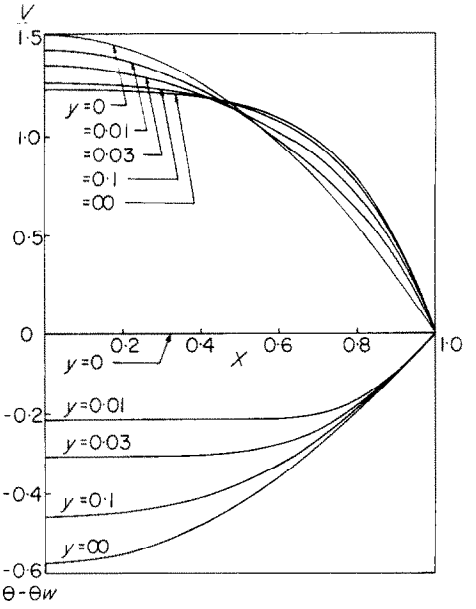

FIG. 2. Developing velocity and temperature profiles for constant heat flux case and $M = 4$, $Gr/Re = 10$, $Pr = e = 1$, $Ec = 0$.

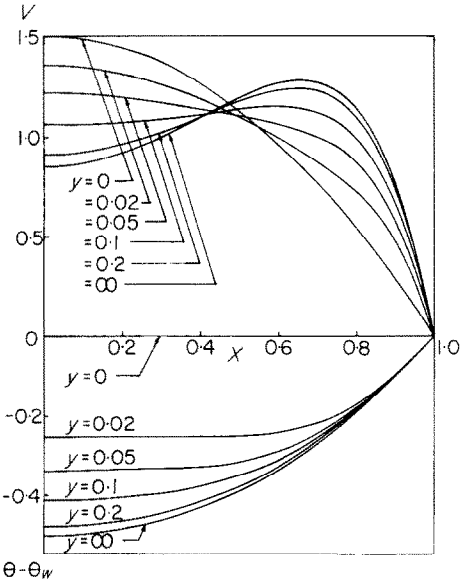

FIG. 3. Developing velocity and temperature profiles for constant heat flux case and $M = 4$, $Gr/Re = 100$, $Pr = e = 1$, $Ec = 0$.

In Fig. 5, the effect of the dissipations is illustrated. By comparing Fig. 5 and Fig. 3, we can see that the dissipations have a similar effect on the velocity developing as that of free convection. The effect on the temperature profiles by the dissipations is that they give rise to a larger temperature difference between the fluid and the wall, and a smaller temperature gradient

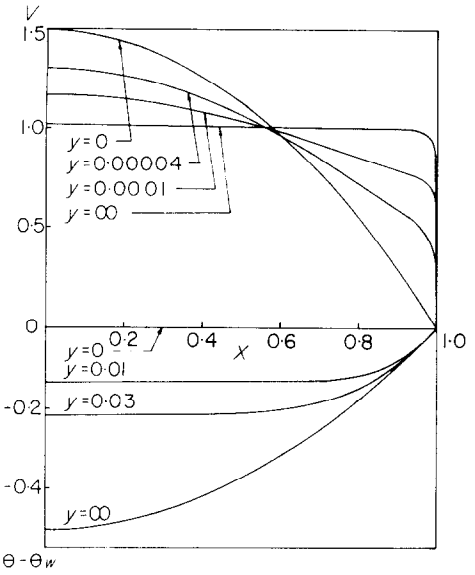

FIG. 4. Developing velocity and temperature profiles for constant heat flux case and $M = 100$, $Gr/Re = 10$, $Pr = e = 1$, $Ec = 0$.

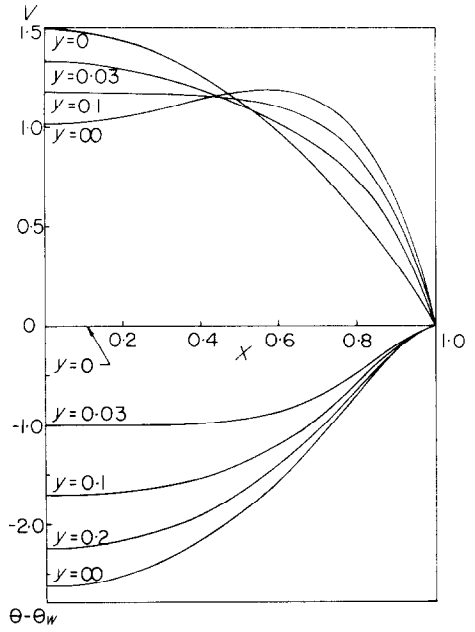

FIG. 5. Developing velocity and temperature profiles for constant heat flux case and $M = 4$, $Gr/Re = 10$, $Pr = e = 1$, $Ec = 1$.

near the wall. This is due to the concentration of the ohmic and viscous heating near the wall where the electric current and velocity gradient are large. As a result of the higher temperature of the fluid near the walls, larger buoyant forces will arise at that region to accelerate the flow.

(B) *Heat transfer of the constant heat flux case*

Some results on heat transfer are presented in this section in terms of the local Nusselt number. In Fig. 6, Nu is plotted for different values of M and Gr/Re. In general the presence of the magnetic field and free convection both lead to an increase of heat transfer. But the effect of the magnetic field is more important in the entrance region than in the fully developed region. The opposite is true for the free convection effect.

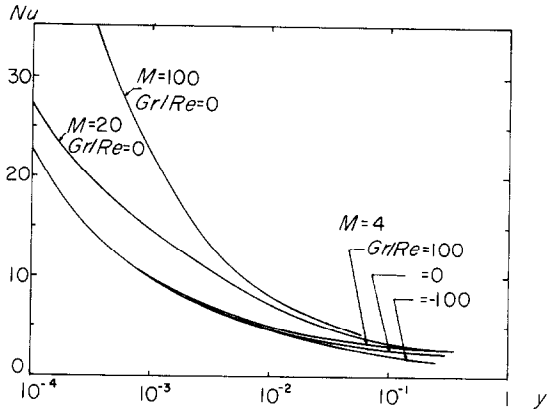

FIG. 6. Local Nusselt number for constant heat flux case, $Pr = e = 1$, $Ec = 0$ and different values of M and Gr/Re.

Table 2 shows a comparison of the heat-transfer results with those obtained by other authors for the case in which free convection is absent. They appear in very good agreement, considering the fact that there is a 1 per cent limit in the calculation.*

Table 2. Comparison of the local Nusselt number at $y \to \infty$ for $Gr = 0$, $Ec = 0$

M	Nu Perlmutter and Siegel [29]	Nu Hwang *et al.* [26]	Present work
4	2·2753	2·2633	2·2892
10	2·5646	2·5504	2·5798

The effect of dissipations on the heat transfer are presented in Fig. 7, where we plot the local Nusselt number for various values of Ec. The effect of dissipations is to decrease the heat transfer as in the case of the fully developed flow [8].

*The results of the present work are obtained for $Pr = 1$ at the location where both velocity and temperature at the center line reach 1 per cent of their fully developed value.

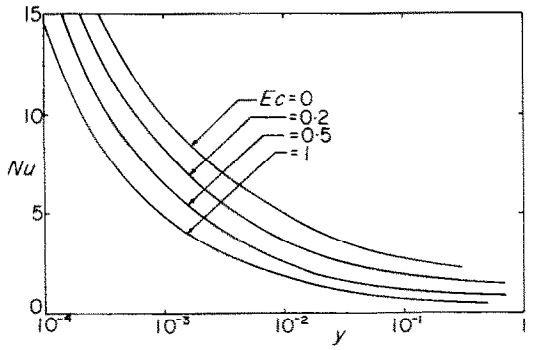

FIG. 7. Local Nusselt number for constant heat flux case, $M = 4, Gr/Re = 10, Pr = e = 1$ and different values of Ec.

(C) *Pressure gradient and friction factor of the constant heat flux case*

In Fig. 8, the modified pressure gradient

$$\nabla Pm\left(=\frac{\mathrm{d}p}{\mathrm{d}y}-\frac{Gr}{RePr}y\right),$$

which is constant in the fully developed flow, is plotted against y for different values of M. The jumped pressure gradient at the entrance due to the applied magnetic field are gradually disappeared as the flow proceeds downstream. The larger the value of M, the steeper the jump of the pressure gradient and the faster it reaches to the fully developed state.

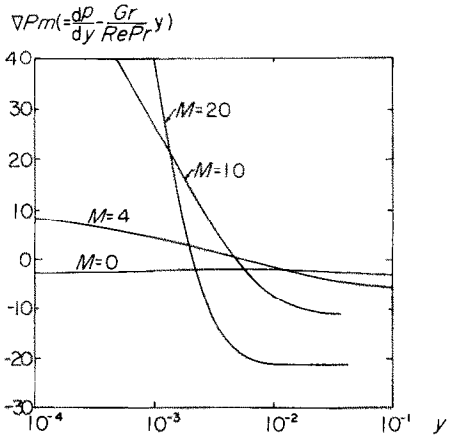

FIG. 8. Modified pressure gradient vs. y for constant heat flux case, $Gr/Re = 10$, $Pr = 0{\cdot}1$, $e = 1$, $Ec = 0$ and different values of M.

The friction factor, revealed by

$$\left.\frac{\mathrm{d}v}{\mathrm{d}x}\right|_{x=1},$$

is shown in Fig. 9. It follows about the same pattern as the modified pressure gradient.

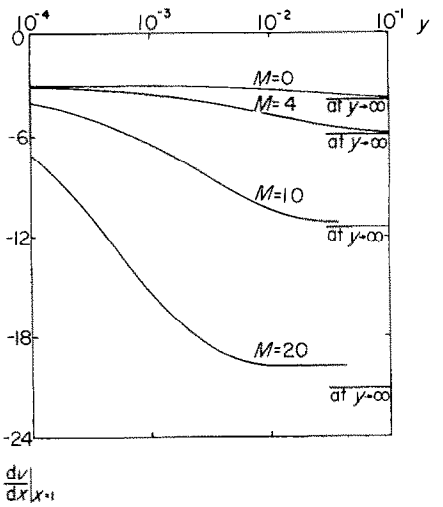

FIG. 9. Velocity gradient at the wall vs. y for constant heat flux case, $Gr/Re = 10$, $Pr = 0{\cdot}1$, $e = 1$, $Ec = 0$ and different values of M.

(D) *Entrance lengths of the constant heat flux case*

As we have already observed previously from the study of the velocity and temperature profiles that an applied magnetic field can greatly reduce the entrance length for the velocity development while it has little effect on the temperature development. This can be seen more easily in Figs. 10 and 11. The entrance lengths for the velocity and temperature development are plotted against M^2 for different values of Gr/Re and Pr. At large M, the entrance length for velocity is approximately inversely proportion to M^2 as it was predicted by Shercliff [6] in the isothermal case. For $M > 20$ the relation can be approximated by the equation

$$y_e = \frac{4{\cdot}3}{M^2}.$$

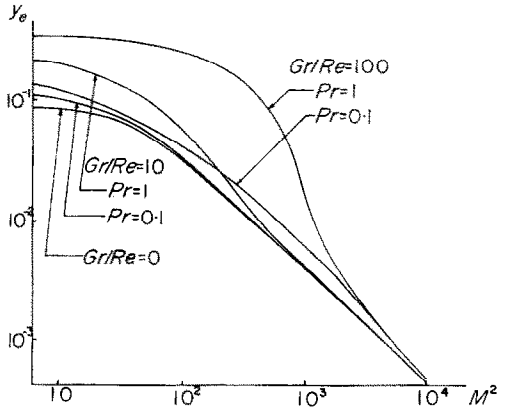

FIG. 10. Velocity entrance lengths vs. M^2 for constant heat flux case, $e = 1$, $Ec = 0$ and different values of Gr/Re and Pr.

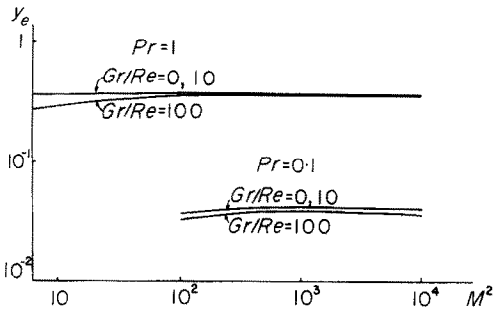

FIG. 11. Thermal entrance lengths vs. M^2 for constant heat flux case, $e = 1$, $Ec = 0$ and different values of Gr/Re and Pr.

However, the deviation to this asymptotic value will be greater when the value of Gr/Re increases. For small M, increasing Gr/Re and Pr increases the entrance length.

For the special case $Gr = 0$, there has been some results of velocity entrance length available in the literature. Table 2 shows a comparison of these results with the present results.

Table 3. Comparison of the velocity entrance length for $Gr = Ec = 0$ (based on 1 per cent deviation of the center velocity)

M	Hwang *et al.* [25]	Flores and Recuero [28]	Present work
2·5	0·0844	0·0858	0·0868
4	0·0722	0·0808	0·0838
10	0·0292	0·0276	0·0319
20	0·0011	0·0012	0·0017

Flores and Recuero [28] claimed that the deviation between their results and those of Hwang's is due to the different imposed initial condition of u. In [25] the results were based on $u = 0$ at the entrance whereas [28] used an initial condition that satisfies the governing equations for the entrance flow under the boundary-layer approximation. The authors tried both conditions on the same program, little difference in the result was found. Therefore, it must be concluded that the deviation of the numerical results are largely due to the different numerical approach rather than the initial condition of u.

Figure 12 shows the entrance lengths plotted against Pr for $M = 0$ and 4. When $Pr > 1$, both the velocity and temperature entrance lengths are about linear proportion to Pr. However when $Pr < 0{\cdot}1$, little change is observed.

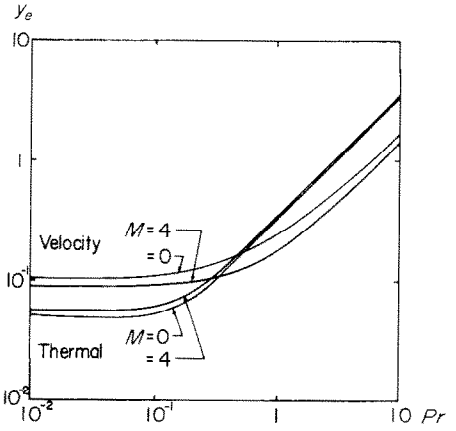

FIG. 12. Entrance lengths vs. Pr for constant heat flux case, $Gr/Re = 10$, $e = 1$, $Ec = 0$ and different values of M.

(E) *Constant wall temperature case*

For the case of constant temperature at wall, the general trend of the velocity and temperature development is similar to that of the constant heat flux case discussed earlier. We shall briefly discuss the results in this section. In Fig. 13 a typical set of the velocity profiles

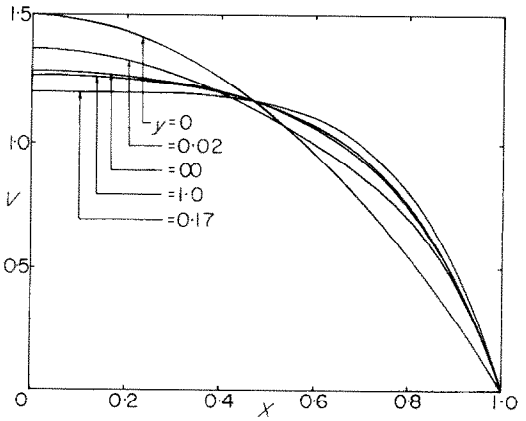

FIG. 13. Developing velocity profiles for constant wall temperature case and $M = 4$, $Gr/Re = 10$, $Pr = e = 1$, $Ec = 0$.

are presented. Since the fully developed velocity profile for the constant wall temperature condition is independent of the parameter Gr/Re, the velocity profile has to readjust itself when it develops from one uniform temperature to another uniform temperature. This explains the seemingly unorthodox phenomenon of "over-shoot" in the figure.

Figure 14 shows a typical set of the developing temperature profiles. It follows pretty much the same pattern as in the constant heat flux case, but the path

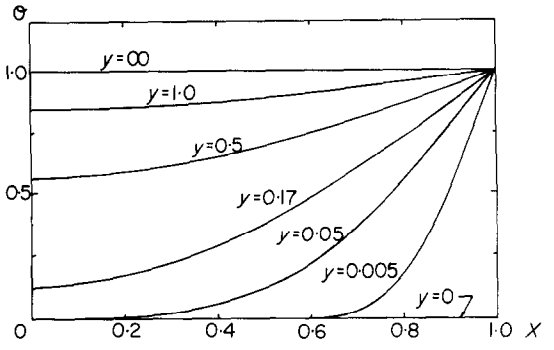

FIG. 14. Developing temperature profiles for constant wall temperature case and $M = 4$, $Gr/Re = 10$, $Pr = e = 1$, $Ec = 0$.

of the developing is much longer than the constant heat flux case. Similar situation occurs for the velocity development.

In Fig. 15, the local heat transfer is compared for the two cases for different values of M. The constant heat flux case usually gives a larger heat-transfer rate, except in the very beginning where the sudden temperature change results in a bigger heat-transfer rate for the constant wall temperature case.

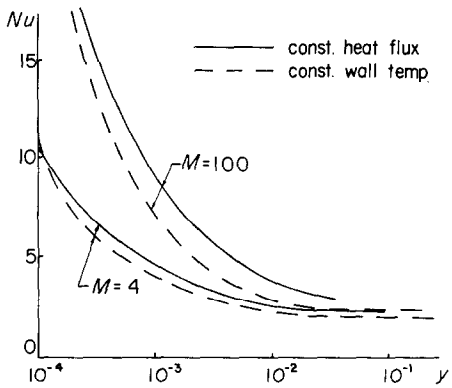

FIG. 15. Comparison of local Nusselt number for $Gr/Re = 10$, $Pr = 0{\cdot}1$, $e = 1$, $Ec = 0$ and different values of M.

The effect of the dissipations on heat transfer is shown in Fig. 16. When the dissipations are sufficiently large, the fluid temperature at beginning is smaller than that of the walls, but it finally exceeds the wall temperature. Thus, the Nusselt number reverses sign after a distance and the heat is transferred from the fluid to the walls. As the distance further increases, a point is reached where the Nusselt number approaches infinity. At this point the mean temperature of the fluid is equal to the wall temperature. Beyond this point the Nusselt number is again positive as both

$$\theta_w - \theta_m \quad \text{and} \quad \left.\frac{\partial\theta}{\partial x}\right|_{x=1} \quad \text{reverse sign.}$$

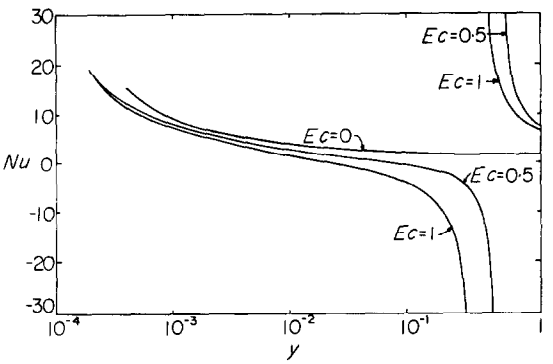

FIG. 16. Local Nusselt number for constant wall temperature case, $M = 4$, $Gr/Re = 10$, $Pr = e = 1$ and different values of Ec.

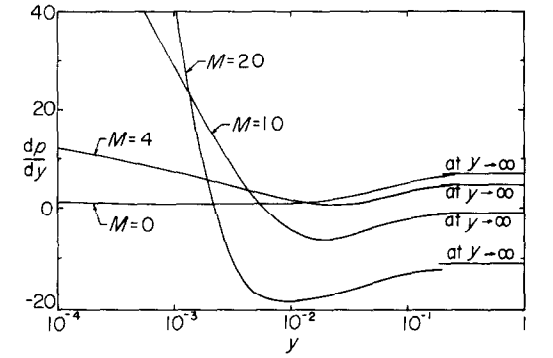

FIG. 17. Pressure gradient vs. y for constant wall temperature case, $Gr/Re = 10$, $Pr = 0{\cdot}1$, $e = 1$, $Ec = 0$ and different values of M.

The local pressure gradient in the entrance region is plotted in Fig. 17 for different values of M. The readjusting of the flow can be also seen from the behavior of the pressure gradient.

Acknowledgements—All numerical computations were conducted at the computing center of the State University of New York at Buffalo. This work was supported in part by the State University of New York Research Foundation.

REFERENCES

1. R. A. Regirer, On convective motion of a conducting fluid between parallel vertical plates in a magnetic field, *Soviet Phys. JETP* **37**, 149 (1959).
2. Y. Mori, On combined free and forced convective laminar magnetohydrodynamic flow and heat transfer in channels with transverse magnetic field, *Int. Dev. Heat Transfer* **5**, 1031 (1961).
3. C. P. Yu, Combined forced and free convection channel flows in magnetohydrodynamics, *AIAA J* **3**, 1184 (1965).
4. R. M. Singer, Combined thermal convective magnetohydrodynamic flow, *Appl. Scient. Res.* **B12**, 375 (1966).
5. C. P. Yu, Convective magnetohydrodynamic flow in a vertical channel, *Appl. Scient. Res.* **22**, 127 (1970).

6. J. Srinivasan, Combined natural and forced convection hydromagnetic flow between electrically conducting walls, *Appl. Scient. Res.* **B11**, 361 (1965).
7. C. P. Yu and H. K. Yang, Effect of wall conductances on convective magnetohydrodynamic channel flow, *Appl. Scient. Res.* **20**, 16 (1969).
8. H. K. Yang and C. P. Yu, Dissipative effect on convection MHD channel flow, *Appl. Scient. Res.* (to be published).
9. J. A. Shercliff, Entry of conducting and non-conducting fluids in pipes, *Proc. Camb. Phil. Soc.* **52**, 573 (1956).
10. J. A. Shercliff, The flow of conducting fluids in circular pipes under transverse magnetic fields, *J. Fluid Mech.* **1**, 644 (1956).
11. H. Schlichting, Laminare Kanaleinlaufstromung, *Z. Angew. Math. Mech.* **14**, 368 (1934).
12. M. Roidt and R. D. Cess, An approximate analysis of laminar MHD flow in the entrance region of a flat duet, *J. Appl. Mech.* **84**, 171 (1962).
13. W. S. Saric and K. J. Touryan, Incompressible magnetohydrodynamic entrance flow in a plane channel, *Physics Fluids* **12**, 1412 (1969).
14. A. M. Phanak, Heat transfer in MHD flow in an entrance section, *J. Heat Transfer* **87**, 231 (1964).
15. A. Maciulaitis and A. L. Loeffler, Jr., A theoretical investigation of MHD channel entrance flow, *AIAA Jl* **2**, 2100 (1964).
16. W. C. Moffatt, Analysis of MHD channel entrance flow using the momentum integral method, *AIAA Jl* **2**, 1495 (1964).
17. E. S. Hsia, Entrance development of the weekly interacted MHD plane channel flow as affected by wall conductances, *J. Appl. Mech.* **38**, 665 (1971).
18. E. M. Sparrow, S. H. Lin and T. S. Lundgren, Flow development in the hydrodynamic entrance region of tubes and ducts, *Physics Fluids* **7**, 338 (1964).
19. W. T. Snyder, Magnetohydrodynamic flow in the entrance region of a parallel-plate channel, *AIAA Jl* **3**, 1833 (1965).
20. T. S. Chen and G. L. Chen, Magnetohydrodynamic channel flow with an arbitrary inlet velocity profile, *Physics Fluids* **15**, 1531 (1972).
21. C. C. Hwang, Linearized analysis of magnetohydrodynamic channel entrance flow, *Physics Fluids* **15**, 1852 (1972).
22. J. L. Shohet, Velocity and temperature profiles for laminar magnetohydrodynamic flow in the entrance region of channels, Ph.D. Thesis, Carnegie Institute of Technology (1961).
23. J. L. Shohet, J. F. Osterle and F. J. Young, Velocity and temperature profiles for laminar MHD flow in the entrance region of a plane channel, *Physics Fluids* **5**, 545 (1962).
24. C. L. Hwang and F. T. Fan, A finite difference analysis of laminar magnetohydrodynamic flow in the entrance region of a flat rectangular duct, *Appl. Scient. Res.* **B10**, 329 (1963).
25. C. L. Hwang, K. C. Li and L. T. Fan, magnetohydrodynamic channel entrance flow with parabolic velocity at the entry, *Physics Fluids* **9**, 1134 (1966).
26. C. L. Hwang, P. J. Knieper and L. T. Fan, Heat transfer to MHD flow in the thermal entrance region of a flat duet, *Int. J. Heat Mass Transfer* **9**, 773 (1966).
27. L. T. Fan, C. L. Hwang, P. J. Kniepper and U. P. Hwang, Heat transfer on magnetohydrodynamic flow in the entrance region of a flat duct, *Z. Angew. Math. Phys.* **18**, 826 (1967).
28. F. Flores and A. Recuero, Magnetohydrodynamic entrance flow in a channel, *Appl. Scient. Res.* **25**, 403 (1972).
29. M. Perlmutter and R. Siegel, Heat transfer to an electrically conducting fluid flowing in a channel with a transverse magnetic field, NASA TN D-875 (1961).

CONVECTION MIXTE EN MHD DANS LA REGION D'ENTREE D'UNE CONDUITE

Résumé—On étudie numériquement le problème magnétohydrodynamique d'un écoulement entre deux plans parallèles et soumis à la fois à des gradients axiaux de température et de pression. On considère les cas de flux pariétal constant et de température constante. Les solutions tendent vers celles pleinement développées au bout d'une certaine longueur d'entrée. On montre que le champs magnétique transverse appliqué peut réduire considérablement la longueur d'établissement dynamique, mais qu'il a un faible effet sur le développement thermique. Aux grands nombres de Hartmann, la longueur d'établissement dynamique est inversement proportionnelle à M^2, comme prévu par Shercliff en l'absence de convection naturelle. Néanmoins une convection naturelle suffisamment forte peut prolonger considérablement le processus de développement.

KOMBINATION VON ERZWUNGENER UND FREIER KONVEKTION MAGNETO-HYDRODYNAMISCHE -KANALSTRÖMUNG IM EINLAUF

Zusammenfassung—Das Einlaufproblem konvektiver magneto-hydrodynamischer Kanalströmung zwischen zwei parallelen Platten in Abhängigkeit von einem gleichzeitigen axialen Temperatur- und Druckgradienten wird numerisch untersucht. Sowohl der Fall mit Wärmefluß, als auch der mit konstanter Wandtemperatur wird betrachtet. Die Ergebnisse stimmen mit den vollständig abgeleiteten Lösungen nach einer bestimmten Einlauflänge überein. Es ergibt sich, daß ein quer angelegtes Magnetfeld die Einlauflänge der Geschwindigkeit beträchtlich verringern kann, jedoch auf die Temperaturentwicklung nur geringe Auswirkungen hat. Bei hoher Hartmann-Zahl ist die Einlauflänge der Geschwindigkeit umgekehrt proportional M^2, wie bei Nichtvorhandensein freier Konvektion von Shercliff belegt wird. Eine genügend starke freie Konvektion kann jedoch den Einlaufvorgang erheblich verlängern.

О МАГНИТОГИДРОДИНАМИЧЕСКОМ ТЕЧЕНИИ ВО ВВОДНОМ УЧАСТКЕ КАНАЛА С СОВМЕСТНОЙ ВЫНУЖДЕННОЙ И СВОБОДНОЙ КОНВЕКЦИЕЙ

Аннотация — Численно решается задача о магнитогидродинамическом течении во входном участке канала, образованного двумя параллельными пластинами, при одновременном изменении аксиального градиента температуры и давления. Рассматриваются случаи как для постоянного теплового потока, так и для постоянной температуры стенки. Полученные решения соответствуют решениям для полностью развитого течения далеко от входа. Найдено что наложенное поперечное магнитное поле может значительно уменьшить скорость во входном участке, но мало влияет на изменение температуры. При высоких числах Гартмана скорость во входном участке обратно пропорциональна M^2, как это и было получено Шерклиффом для случая, когда отсутствует свободная конвекция. Однако, при наличии довольно большой свободной конвекции развитие течения может быть затянуто вниз по потоку.